

# Comparative transcriptome analyses of a late-maturing mandarin mutant and its original cultivar reveals gene expression profiling associated with citrus fruit maturation

Wang Lu<sup>1,2</sup>, Hua Qingzhu<sup>1</sup>, Ma Yuwen<sup>1</sup>, Hu Guibing<sup>1</sup>, Qin Yonghua<sup>Corresp. 1</sup>

<sup>1</sup> State Key Laboratory for Conservation and Utilization of Subtropical Agro-bioresources/Key Laboratory of Biology and Genetic Improvement of Horticultural Crops-South China, Ministry of Agriculture, College of Horticulture, South China Agricultural University, Guangzhou, China

<sup>2</sup> Yunnan Key Laboratory for Wild Plant Resources/Key Laboratory for Economic Plants and Biotechnology, Kunming Institute of Botany, Chinese Academy of Sciences, Kunming, China

Corresponding Author: Qin Yonghua  
Email address: qinyh@scau.edu.cn

Characteristics of late maturity in fruits are good agronomic traits for extending the harvest period and marketing time. However, underlying molecular basis of the late-maturing mechanism in fruit is largely unknown. In this study, RNA sequencing (RNA-Seq) technology was used to identify differentially expressed genes (DEGs) related to late-maturing characteristics from a late-maturing mutant 'Huawan Wuzishatangju' (HWWZSTJ) (*Citrus reticulata* Blanco) and its original line 'Wuzishatangju' (WZSTJ). A total of approximately 17.0 Gb and 84.2 M paired-end reads were obtained. DEGs were significantly enriched in the pathway of photosynthesis, phenylpropanoid biosynthesis, carotenoid biosynthesis, chlorophyll and abscisic acid (ABA) metabolism. Thirteen candidate transcripts related to chlorophyll metabolism, carotenoid biosynthesis and ABA metabolism were analyzed using real-time quantitative PCR (qPCR) at all fruit maturing stages of HWWZSTJ and WZSTJ. Chlorophyllase (*CLH*) and divinyl reductase (*DVR*) from chlorophyll metabolism, phytoene synthase (*PSY*) and capsanthin/capsorubin synthase (*CCS*) from carotenoid biosynthesis, abscisic acid 8'-hydroxylase (*AB1*) and 9-cis-epoxycarotenoid dioxygenase (*NCED1*) from ABA metabolism were cloned and analyzed. The expression pattern of *NCED1* indicates its role in the late-maturing characteristics of HWWZSTJ. There were 270 consecutive bases missing in HWWZSTJ in comparison with full-length sequences of *NCED1* cDNA from WZSTJ. Those results suggested that *NCED1* might play an important role in late maturity of HWWZSTJ. This study provides new information of complex process that results in late maturity of *Citrus* fruit at the transcriptional level.

1 **Comparative transcriptome analyses of a late-maturing mandarin mutant and its original**  
2 **cultivar reveals gene expression profiling associated with citrus fruit maturation**

3 Wang Lu<sup>1,2</sup>, Hua Qingzhu<sup>1</sup>, Ma Yuewen<sup>1</sup>, Hu Guibing<sup>1</sup>, QinYonghua<sup>1\*</sup><sup>1</sup>

4 <sup>1</sup>State Key Laboratory for Conservation and Utilization of Subtropical Agro-bioresources/Key  
5 Laboratory of Biology and Genetic Improvement of Horticultural Crops-South China, Ministry  
6 of Agriculture, College of Horticulture, South China Agricultural University, Guangzhou, China.

7 <sup>2</sup>Yunnan Key Laboratory for Wild Plant Resources/Key Laboratory for Economic Plants and  
8 Biotechnology, Kunming Institute of Botany, Chinese Academy of Sciences, Kunming, China.

9

10 **Abstract**

11 Characteristics of late maturity in fruits are good agronomic traits for extending the harvest  
12 period and marketing time. However, underlying molecular basis of the late-maturing  
13 mechanism in fruit is largely unknown. In this study, RNA sequencing (RNA-Seq) technology  
14 was used to identify differentially expressed genes (DEGs) related to late-maturing  
15 characteristics from a late-maturing mutant ‘Huawan Wuzishatangju’ (HWWZSTJ) (*Citrus*  
16 *reticulata* Blanco) and its original line ‘Wuzishatangju’ (WZSTJ). A total of approximately 17.0  
17 Gb and 84.2 M paired-end reads were obtained. DEGs were significantly enriched in the  
18 pathway of photosynthesis, phenylpropanoid biosynthesis, carotenoid biosynthesis, chlorophyll  
19 and abscisic acid (ABA) metabolism. Thirteen candidate transcripts related to chlorophyll  
20 metabolism, carotenoid biosynthesis and ABA metabolism were analyzed using real-time  
21 quantitative PCR (qPCR) at all fruit maturing stages of HWWZSTJ and WZSTJ. Chlorophyllase  
22 (*CLH*) and divinyl reductase (*DVR*) from chlorophyll metabolism, phytoene synthase (*PSY*) and  
23 capsanthin/capsorubin synthase (*CCS*) from carotenoid biosynthesis, abscisic acid 8'-hydroxylase  
24 (*ABI*) and 9-cis-epoxycarotenoid dioxygenase (*NCEDI*) from ABA metabolism were cloned and  
25 analyzed. The expression pattern of *NCEDI* indicates its role in the late-maturing characteristics

---

\*Corresponding author. E-mail address: qinyh@scau.edu.cn.

26 of HWWZSTJ. There were 270 consecutive bases missing in HWWZSTJ in comparison with  
27 full-length sequences of *NCEDI* cDNA from WZSTJ. Those results suggested that *NCEDI*  
28 might play an important role in late maturity of HWWZSTJ. This study provides new  
29 information of complex process that results in late maturity of *Citrus* fruit at the transcriptional  
30 level.

31

## 32 **Introduction**

33 Fruit maturity date is an important economic trait and selection of varieties with different  
34 harvest time would be advantageous to extend their storage period and market share. Citrus, one  
35 of the most important fruit crops, is large-scale commercial production in the tropical and  
36 subtropical regions of the world. The total harvested area of citrus exceeds 8.8 million ha, with  
37 an annual yield of over 130 million tons in 2015 (FAOSTAT, 2014). Currently, harvest time for  
38 most citrus is mainly from November to December resulting in huge market pressure. Therefore,  
39 breeding of early- and late-maturing citrus varieties is essential to extend marketing season, meet  
40 the needs of consumers and ensure an optimal adaptation to climatic and geographic conditions.

41 Plant hormones play important roles in the regulation of fruit development and ripening  
42 (Kumar et al., 2014). Ethylene is known to be the major hormonal regulator in climacteric fruit  
43 ripening. In addition to ethylene, abscisic acid (ABA), auxin, gibberellin (GA) and  
44 brassinosteroid are involved in regulating fruit ripening. ABA plays an important role as an  
45 inducer along with ethylene signaling for the onset of fruit degreening and carotenoid  
46 biosynthesis during development and ripening process in climacteric and non-climacteric fruits  
47 (Leng et al., 2009; Sun et al., 2010; Jia et al., 2011; Romero et al., 2012; Soto et al., 2013; Wang  
48 et al., 2016). ABA treatment can rapidly induced flavonol and anthocyanin accumulation in berry  
49 skins of the *Cabernet Sauvignon* grape suggesting that ABA could stimulate berry ripening and  
50 ripening-related gene expression (Koyama et al., 2010). ABA also participated in the regulation  
51 of fruit development and ripening of tomato (Zhang et al., 2009b; Sun et al., 2011), cucumber  
52 (Wang et al., 2013), strawberry (Jia et al., 2011), bilberry (Karppinen et al., 2013), citrus (Zhang

53 et al., 2014) and grape (Nicolas et al., 2014). Recent studies showed that ABA is a positive  
54 regulator of ripening and exogenous ABA application could effectively regulate citrus fruit  
55 maturation (Wang et al., 2016). Those results suggest that ABA metabolism plays a crucial role  
56 in the regulation of fruit development and ripening. In addition, fruit deterioration and post  
57 harvest processes might influence fruit quality and ripening process. However, there were  
58 few reports involved in those processes.  $\alpha$ -mannosidase ( $\alpha$ -Man) and  $\beta$ -D-N-  
59 acetylhexosaminidase ( $\beta$ -Hex) are the two ripening-specific N-glycan processing enzymes have  
60 been proved that their transcripts increased with the in non-climacteric fruit ripening and  
61 softening (Ghosh et al., 2011). Genetic results have proved that 9-cis-epoxycarotenoid  
62 dioxygenase (NCED) is the key enzyme in ABA metabolism in plants (Liotenberg et al., 1999;  
63 Luchi et al., 2001). *NCED1* could initiate ABA biosynthesis at the beginning of fruit ripening in  
64 both peach and grape fruits (Zhang et al., 2009a). Silence of *FaNCED1* (encoding a key ABA  
65 synthesis enzyme) in strawberry fruit could cause the ABA levels decreased significantly and  
66 uncolored fruits and this phenomenon could be rescued by application of exogenous ABA (Jia et  
67 al., 2011). Suppression of the expression of *SLNCED1* could result in delay of fruit softening and  
68 maturation in tomato (Sun et al., 2012). Overexpression of ABA-response element binding  
69 factors (*SlAREB1*) in tomato could regulate organic acid and sugar contents during tomato fruit  
70 development. Higher levels of organic acid, sugar contents and related-gene expression were  
71 detected in *SlAREB1*-overexpressing lines in fruit pericarp of mature tomato (Bastías et al.,  
72 2014). However, there is little information available about the role of *NCED1* genes in citrus  
73 fruit maturation (Zhang et al., 2014).

74 Bud mutant selection is the most common method for creating novel cultivars in *Citrus*.  
75 ‘Huawan Wuzishatangju’ (HWWZSTJ) mandarin is an excellent cultivar derived from a bud  
76 sport of a seedless cultivar ‘Wuzishatangju’ (WZSTJ). Fruits of HWWZSTJ are mature in late  
77 January to early February of the following year, which is approximately 30 d later than WZSTJ  
78 (Qin et al., 2013; Qin et al., 2015). Therefore, the late-maturing mutant and its original cultivar  
79 are excellent materials to identify and describe the molecular mechanism involved in citrus fruit

80 maturation. In this study, the high efficient RNA-Seq technology was used to identify  
81 differentially expressed genes (DEGs) between the late-maturing mutant HWWZSTJ and its  
82 original line WZSTJ mandarins. DEGs involved in carotenoid biosynthesis, chlorophyll  
83 degradation and ABA metabolism were characterized. The present work could help to reveal the  
84 molecular mechanism of late-maturing characteristics of citrus fruit at the transcriptional level.

## 85 **Materials&Methods**

### 86 **Plant Materials**

87 The late-maturing mutant ‘Huawan Wuzishatangju’ (HWWZSTJ) (*Citrus reticulata* Blanco)  
88 and its original cultivar ‘Wuzishatangju’ (WZSTJ) were planted in the same orchard in South  
89 China Agricultural University (23°09’38”N, 113°21’13”E). Ten six-year-old trees of each  
90 cultivar were used in this experiment. Peels (including albedo and flavedo fractions) from fifteen  
91 uniform-sized fresh fruits were collected on the 275<sup>th</sup> (color-break stage, i.e. peels turns from  
92 green to orange) and 320<sup>th</sup> (maturing stage) days after flowering (DAF) of HWWZSTJ an 275<sup>th</sup>  
93 (maturing stage) DAF of WZSTJ ( **Fig. S1**) in 2012 and pools were named T3, T1 and T2,  
94 respectively. Peels from fifteen uniform-sized fresh fruits of HWWZSTJ and WZSTJ were  
95 collected on the 255<sup>th</sup>, 265<sup>th</sup>, 275<sup>th</sup>, 285<sup>th</sup>, 295<sup>th</sup>, 305<sup>th</sup>, 315<sup>th</sup> and 320<sup>th</sup> DAF in 2012 and used for  
96 expression analyses of candidate transcripts associated with chlorophyll, carotenoid biosynthesis  
97 and ABA metabolism. All samples were immediately frozen in liquid nitrogen and stored at -80  
98 °C until use.

### 99 **RNA Extraction, Library Construction and RNA-Seq**

100 Total RNA was extracted from peels according to the protocol of the RNAout kit (Tiandz,  
101 Beijing, China) and genomic DNA was removed by DNase I (TaKaRa, Dalian, China). RNA  
102 quality was analyzed by 1.0% agarose gel and its concentration was quantified by a NanoDrop  
103 ND1000 spectrophotometer (NanoDrop Technologies, Wilmington, DE, USA). RNA integrity  
104 number (RIN) values (>7.0) were assessed using an Agilent 2100 Bioanalyzer (Agilent  
105 Technologies, Santa Clara, CA, USA).

106 Construction of RNA-Seq libraries was performed by the Biomarker Biotechnology  
107 Corporation (Beijing, China). mRNA was enriched and purified with oligo (dT)-rich magnetic  
108 beads and then broken into short fragments. The cleaved RNA fragments were reversely  
109 transcribed to the first-strand cDNA using random hexamer primers. The second-strand cDNA  
110 was synthesized using RNase H and DNA polymerase I. The cDNA fragments were purified,  
111 end blunted, 'A' tailed, and adaptor ligated. The distribution sizes of the cDNA in the three  
112 libraries were monitored using an Agilent 2100 bioanalyzer. Finally, the three libraries were  
113 sequenced using an Illumina HiSeq™ 2500 platform.

#### 114 Transcriptome Assembly and Annotation

115 Sequences obtained in this study were annotated in reference to the genome sequence of  
116 *Citrus sinensis* (Xu et al., 2013; Wang et al., 2014) using a TopHat program (Trapnell et al.,  
117 2009). Functional annotation of the unigenes was performed using BLASTx (Altschul et al.,  
118 1997) and classified by Swiss-Prot (SWISS-PROT downloaded from European Bioinformatics  
119 Institute by Jan., 2013), Clusters of Orthologous Groups of Proteins Database (COG) (Tatusov et  
120 al., 2000), Kyoto Encyclopedia of Genes and Genomes Database (KEGG, release 58) (Kanehisa  
121 et al., 2004), non-redundant (nr) (Deng et al., 2006) and Gene Ontology (GO) (Harris et al.,  
122 2004). The number of mapped and filtered reads for each unigene was calculated and normalized  
123 giving the corresponding Reads Per Kilobases per Million reads (RPKM) values. DEGs between  
124 the two samples were determined according to a false discovery rate (FDR) threshold of < 0.01,  
125 an absolute log<sub>2</sub> fold change value of  $\geq 2$  and a P-value < 0.01.

#### 126 Gene Validation and Expression Analysis

127 Data from RNA-Seq were validated using qPCR. All pigment-related (chlorophyll  
128 metabolism, carotenoid biosynthesis and ABA metabolism) uni-transcripts were selected to  
129 elucidate their expression patterns at all peel coloration stages of HWWZSTJ and WZSTJ with  
130 specific primers (**Table S1**). The citrus *actin* gene (accession No. GU911361.1) was used as an  
131 internal standard for the normalization of gene expression. Expression levels of all pigment-

132 related uni-transcripts were determined using qPCR in an Applied Biosystems 7500 real-time  
133 PCR system (Applied Biosystems, CA, USA). A total of 20.0  $\mu$ l reaction volume contained 10.0  
134  $\mu$ l THUNDERBIRD SYBR qPCR Mix (TOYOBO Co., Ltd.), 50 $\times$ ROX Reference dye, 2.0  $\mu$ l  
135 Primer Mix (5.0  $\mu$ M), 6.0  $\mu$ l ddH<sub>2</sub>O, and 2.0  $\mu$ l cDNA (40 ng). The qPCR parameters were: 94  
136  $^{\circ}$ C for 60 s then 40 cycles of 95  $^{\circ}$ C for 15 s, 55  $^{\circ}$ C for 15 s and 72  $^{\circ}$ C for 30 s. All experiments  
137 were performed three times with three biological replicates. Relative expression levels of  
138 selected transcripts were calculated by the  $2^{-\Delta\Delta C_T}$  method (Livak & Schmittgen, 2001).

139 All pigment-related genes (chlorophyll metabolism, carotenoid biosynthesis, ABA  
140 metabolism) were cloned using specific primers (**Table S2**). The 20.0  $\mu$ l of reaction volume  
141 contained 2.0  $\mu$ l 10 $\times$ PCR buffer, 2.0  $\mu$ l dNTP (2.0 mM), 0.2  $\mu$ l of each primer (10  $\mu$ M), 2.0  $\mu$ l  
142 DNA (100 ng), 0.2  $\mu$ l LA *Taq* and 13.4  $\mu$ l ddH<sub>2</sub>O. PCR reaction procedure was 94  $^{\circ}$ C for 4 min  
143 then 35 cycles of 94  $^{\circ}$ C for 30 s, 55  $^{\circ}$ C for 30 s and 72  $^{\circ}$ C for 2 min, with a final 72  $^{\circ}$ C for 10 min.  
144 Nucleotide sequences of the pigment-related genes were analyzed using the National Center for  
145 Biotechnology Information (NCBI) Blast program (<http://www.ncbi.nlm.nih.gov/BLAST>). ORFs  
146 were made using the NCBI ORF Finder (<http://www.ncbi.nlm.nih.gov/gorf/gorf.html>).  
147 Alignments were done using ClustalX 1.83 and DNAMAN software. Phylogenetic analysis of  
148 deduced amino acid sequences were performed using MEGA (version 5.0) and the  
149 Neighborjoining method with 1,000 bootstrap replicates.

150

## 151 **Results**

### 152 RNA-Seq Analyses

153 To obtain differentially expressed genes (DEGs) between HWWZSTJ and WZSTJ, three  
154 libraries (T1, T2 and T3) were designed for RNA-Seq. As shown in **Table 1**, 26,403,257,  
155 29,163,126, 28,606,868 raw reads were obtained respectively from the three libraries. After  
156 removing low-quality bases and reads, a total of approximately 17.0 Gb clean reads were  
157 obtained. The GC contents for T1, T2 and T3 were 44.27%, 44.62% and 44.20%, respectively

158 (Table 1). The range of most transcripts length was 100-200 bp (Fig. S2). Q30 percentage  
 159 (percentage of sequences with sequencing error rate lower than 0.01%) for each sample was over  
 160 90% (Table 1).

161

162 **Table 1** Summary of the sequencing data

Samples	Total reads	Total base	GC content (%)	Q30 (%)
T1	26,403,257	5,332,498,617	44.27	94.11
T2	29,163,126	5,890,197,025	44.62	93.98
T3	28,606,868	5,777,864,876	44.20	93.90

163 Note: T1, HWWZSTJ (320 DAF); T2, WZSTJ (275 DAF); T3, HWWZSTJ (275 DAF).

164

165 A total of 44,664,047, 49,507,338 and 48,492,905 reads were mapped which accounted for  
 166 84.58%, 84.88% and 84.76% of the total reads, respectively (Table 2). Number of unique  
 167 mapped reads accounted for 97.14% (T1), 97.25% (T2) and 97.19% (T3) of the total mapped  
 168 reads compared with 2.86% (T1), 2.75% (T2) and 2.81% (T3) for multiple mapped reads,  
 169 respectively. Those results suggested that the throughput and sequencing quality was high  
 170 enough for further analyses.

171

172

173 **Table 2** Summary of the transcriptome annotation compared with the reference genome of

174 *C. Sinensis* (Xu et al., 2013)

Statistics libraries	T1		T2		T3	
	Number	Percentage	Number	Percentage	Number	Percentage
Total reads	52,806,514	100.0%	58,326,252	100.0%	57,213,736	100.0%
Mapped reads	44,664,047	84.58%	49,507,338	84.88%	48,492,905	84.76%
Unique mapped reads	43,386,022	97.14%	48,146,871	97.25%	47,129,445	97.19%
Multiple mapped reads	1,278,025	2.86%	1,360,467	2.75%	1,363,460	2.81%

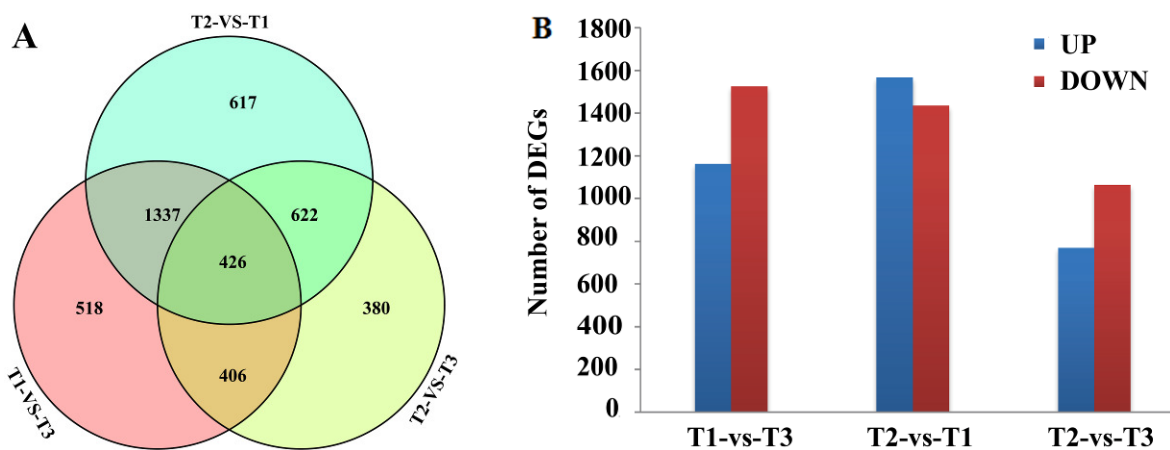
Pair mapped reads	39,251,294	87.88%	43,459,426	87.78%	42,663,447	87.98%
Single mapped reads	4,574,673	10.24%	5,159,966	10.42%	4,969,429	10.25%

175 Note: T1, HWWZSTJ (320 DAF); T2, WZSTJ (275 DAF); T3, HWWZSTJ (275 DAF).

## 176 Analyses of Differentially Expressed Genes (DEGs)

177 DEGs were screened by comparison between any two of the three libraries using  $p \leq 0.01$   
 178 and  $2 \leq \text{fold changes} \leq 5$  as thresholds. A total of 2,687, 3,002 and 1,834 DEGs were obtained  
 179 between the T1 and T3, T2 and T1, T2 and T3 libraries, respectively (**Fig. 1A**). Among those  
 180 DEGs, 1,162, 1,567 and 770 were up-regulated and 1,525, 1,435 and 1,064 were down-regulated  
 181 (**Fig. 1B**). Transcriptional levels of DEGs in HWWZSTJ on 320<sup>th</sup> DAF were lower than that on  
 182 275<sup>th</sup> DAF in HWWZSTJ suggesting that transcriptional levels of DEGs decreased during fruit  
 183 maturation in HWWZSTJ (**Fig. 1B**).

184



185

186 **Figure 1** Venn diagram (A) and histogram (B) of DEGs

187 T1, HWWZSTJ (320 DAF); T2, WZSTJ (275 DAF); T3, HWWZSTJ (275 DAF)

## 188 Functional Annotation of Transcripts

189 A total of 299 new transcripts were annotated using five public databases (Nr, Swiss-Prot,  
 190 KEGG, COG and GO). A summary of the annotations was shown in **Table S3**. Maximum  
 191 number of annotation of differentially expressed transcripts (2,954) was Nr databases by  
 192 comparison between T1 and T3, T2 and T1, T2 and T3, followed by GO databases (2,648)

193 (Table S4). The differentially expressed transcripts were classified into three categories in GO  
 194 assignments: cellular component, molecular function and biological process. DEGs between T1  
 195 and T3, T2 and T1, T2 and T3 were all significantly enriched in pigmentation, signaling and  
 196 growth biological processes (Fig. S3A). Based on COG classifications, differentially expressed  
 197 transcripts were divided into 25 different functional groups (Fig. S3B). DEGs between any two  
 198 of the three libraries (T1-VS-T3, T2-VS-T1, T2-VS-T3) were assigned to 91, 100 and 91 KEGG  
 199 pathways, respectively (File S1), and phenylalanine metabolism, porphyrin and chlorophyll  
 200 metabolism, and flavonoid biosynthesis were the three most significantly enriched biological  
 201 processes (Table 3).

202

203

**Table 3** Analyses of differentially expressed transcripts based on KEGG pathway

#	Pathway	DEGs with	All genes with	p_value	corr_p_	Pathway
		pathway	pathway			
		annotation	annotation		value	ID
		(283)	(3516)			
1	Phenylpropanoid biosynthesis	24 (8.48%)	82 (2.33%)	9.58e-09	8.71e-07	ko00940
2	Photosynthesis	14 (4.95%)	46 (1.31%)	7.90e-06	7.19e-04	ko00195
3	Plant-pathogen interaction	26 (9.19%)	130 (3.7%)	8.30e-06	7.56e-04	ko04626
4	Plant hormone signal transduction	31 (10.95%)	180 (5.12%)	2.73e-05	2.49e-03	ko04075
5	Phenylalanine metabolism	17 (6.01%)	72 (2.05%)	3.59e-05	3.26e-03	ko00360
T1	6 Photosynthesis-antenna proteins	7 (2.47%)	15 (0.43%)	7.45e-05	6.78e-03	ko00196
vs	7 Galactose metabolism	10 (3.53%)	45 (1.28%)	2.46e-03	2.23e-01	ko00052
T3	8 Starch and sucrose metabolism	21 (7.42%)	137 (3.9%)	2.66e-03	2.42e-01	ko00500
9	Porphyrin and chlorophyll metabolism	8 (2.83%)	37 (1.05%)	7.83e-03	7.12e-01	ko00860
10	Amino sugar and nucleotide sugar metabolism	14 (4.95%)	89 (2.53%)	1.06e-02	9.66e-01	ko00520

	1	Photosynthesis	18 (5.17%)	46 (1.31%)	1.1384e-07	1.1384e-05	ko00195
	2	Photosynthesis antenna proteins	10 (2.87%)	15 (0.43%)	1.5234e-07	1.5234e-05	ko00196
	3	Plant-pathogen interaction	32 (9.2%)	130 (3.7%)	5.5471e-07	5.5471e-05	ko04626
	4	Phenylpropanoid biosynthesis	22 (6.32%)	82 (2.33%)	7.9820e-06	7.9820e-04	ko00940
	5	Cyanoamino acid metabolism	9 (2.59%)	22 (0.63%)	1.2713e-04	1.2713e-02	ko00460
T2	6	Biosynthesis of unsaturated	9 (2.59%)	29 (0.82%)	1.3656e-03	1.3656e-01	ko01040
vs		fatty acids					
T1	7	Phenylalanine metabolism	16 (4.6%)	72 (2.05%)	1.3850e-03	1.3850e-01	ko00360
	8	Flavonoid biosynthesis	10 (2.87%)	37 (1.05%)	2.3996e-03	2.3996e-01	ko00941
	9	Starch and sucrose metabolism	23 (6.61%)	137 (3.9%)	7.1760e-03	7.1760e-01	ko00500
	10	Stilbenoid, diarylheptanoid and gingerol biosynthesis	5 (1.44%)	14 (0.4%)	8.6944e-03	8.6944e-01	ko00945
	1	Photosynthesis	26 (10.48%)	46 (1.31%)	5.1027e-19	4.6434e-17	ko00195
	2	Photosynthesis-antenna proteins	11 (4.44%)	15 (0.43%)	1.8431e-10	1.6772e-08	ko00196
	3	Phenylpropanoid biosynthesis	24 (9.68%)	82 (2.33%)	6.3286e-10	5.7590e-08	ko00940
	4	Phenylalanine metabolism	16 (6.45%)	72 (2.05%)	2.6448e-05	2.4068e-03	ko00360
	5	Nitrogen metabolism	9 (3.63%)	32 (0.91%)	2.4845e-04	2.2609e-02	ko00910
	6	Flavone and flavonol biosynthesis	6 (2.42%)	15 (0.43%)	3.3744e-04	3.0707e-02	ko00944
T2	7	Cyanoamino acid metabolism	7 (2.82%)	22 (0.63%)	5.4299e-04	4.9412e-02	ko00460
vs							
T3	8	Stilbenoid, diarylheptanoid and gingerol biosynthesis	5 (2.02%)	14 (0.4%)	1.9788e-03	1.8007e-01	ko00945
	9	Glyoxylate and dicarboxylate metabolism	7 (2.82%)	28 (0.8%)	2.6144e-03	2.3791e-01	ko00630
	10	Flavonoid biosynthesis	8 (3.23%)	37 (1.05%)	3.5075e-03	3.1918e-01	ko00941
	11	Porphyrin and chlorophyll metabolism	8 (3.23%)	37 (1.05%)	3.5075e-03	3.1918e-01	ko00860

---

12	Plant-pathogen interaction	18 (7.26%)	130 (3.7%)	3.9071e-03	3.5554e-01	ko04626
----	----------------------------	------------	------------	------------	------------	---------

---

## 204 Verification the Accuracy of the RNA-Seq Data Using qPCR

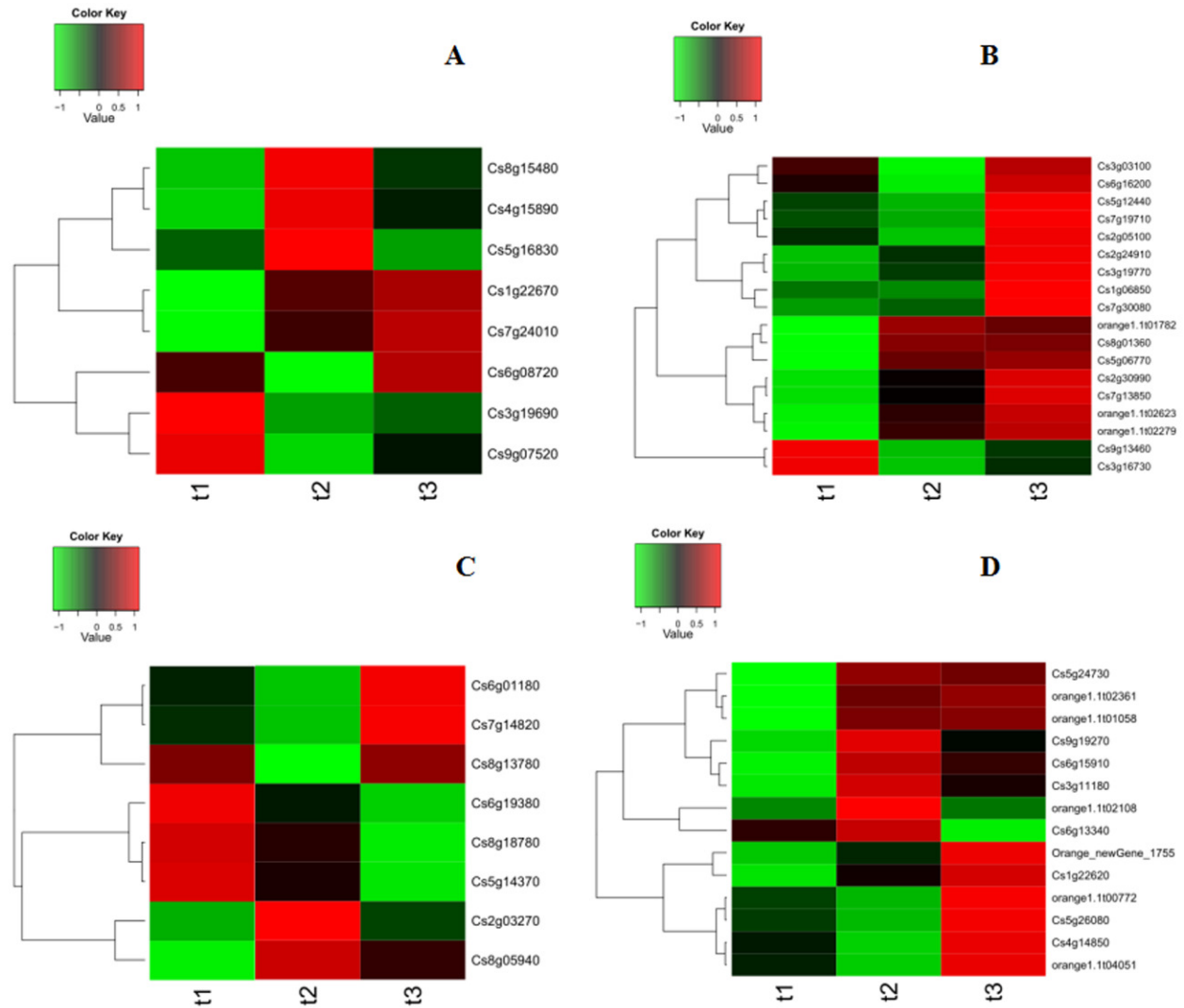
205 Twelve DEGs with significant difference from the three libraries were selected for  
 206 verification of RNA-Seq data by qPCR. Linear regression analysis showed an overall correlation  
 207 coefficient of 0.828, indicating a good correlation between qPCR results and the transcripts per  
 208 kilobase million from the RNA-Seq data (Fig. S4).

209

## 210 DEGs Related to Carotenoid Biosynthesis, Chlorophyll and ABA Metabolism

211 Analyses of the expression data obtained through RNA-Seq revealed that most DEGs were  
 212 involved in carotenoid biosynthesis, chlorophyll and ABA metabolism. The main transcripts  
 213 involved in the three pathways were shown in **Table 4** and heatmap were made based on  
 214 transcripts per kilobase million from the RNA-Seq data (**Fig. 2**). Three transcripts (*Cs8g15480*,  
 215 Pheophorbide a oxygenase; *Cs5g16830*, Chlorophyllase type 0 and *Cs3g19690*, Chlorophyll  
 216 synthase) involved in chlorophyll degradation, six transcripts (*Cs3g19770*, Delta-aminolevulinic  
 217 acid dehydratase; *Cs9g13460*, Magnesium-chelatase subunit H; *Cs2g05100*, Magnesium-  
 218 chelatase subunit ChII-1; *Cs7g19710*, Magnesium-protoporphyrin O-methyltransferase;  
 219 *Cs6g16200*, Magnesium-protoporphyrin IX monomethyl ester [oxidative] cyclase 1 and  
 220 *Cs1g06850*, Protochlorophyllide reductase A) involved in chlorophyll biosynthesis, five  
 221 transcripts (*Cs6g15910*, Phytoene synthase; *Orange1.1t02108*, phytoene synthase 2; *Cs6g13340*,  
 222 Prolycopene isomerase 1; *Cs4g14850/Orange1.1t00772*, Capsanthin/capsorubin synthase and  
 223 *Orange\_new Gene\_1755*, Lycopene beta-cyclase) involved in carotenoid biosynthesis and four  
 224 transcripts (*Cs2g03270/Cs5g14370*, 9-cis-epoxycarotenoid dioxygenase 2; *Cs6g01180*,  
 225 Xanthoxin dehydrogenase; *Cs7g14820*, Carotenoid cleavage dioxygenase 4a and *Cs6g19380*,  
 226 ABA 8'-hydroxylase) involved in ABA metabolism were obtained (**Fig. 2** and **Table 4**).

227



228

229 **Figure 2** Heatmap of main transcripts from chlorophyll metabolism (A), chlorophyll synthesis

230

(B), carotenoid biosynthesis (C) and ABA metabolism (D)

231

232 **Table 4** Analyses of transcripts involved in carotenoid biosynthesis, chlorophyll and ABA

233 metabolism

Gene ID	RPKM			Nr-annotation
	T1	T2	T3	
<b>Chlorophyll metabolism</b>				
<i>Cs3g03100</i>	69.88	63.55	72.16	Probable glutamate-tRNA ligase [ <i>Arabidopsis thaliana</i> ]
<i>Cs8g01360</i>	56.22	59.50	59.42	Glutamate-tRNA ligase 1 [ <i>Arabidopsis thaliana</i> ]

<i>Cs3g16730</i>	78.03	66.88	70.76	Glutamyl-tRNA reductase 1 [ <i>Arabidopsis thaliana</i> ]
<i>Orange1.1t02623</i>	89.64	138.40	164.18	Glutamate-1-semialdehyde 2,1-aminomutase 1, Chloroplastic [ <i>Arabidopsis thaliana</i> ]
<i>Cs3g19770</i>	35.03	42.97	62.68	Delta-aminolevulinic acid dehydratase, chloroplastic [ <i>Arabidopsis thaliana</i> ]
<i>Cs7g13850</i>	16.13	23.66	30.83	Porphobilinogen deaminase [ <i>Arabidopsis thaliana</i> ]
<i>Cs5g12440</i>	21.59	19.34	27.86	Uroporphyrinogen decarboxylase 1, chloroplastic
<i>Cs7g30080</i>	53.66	58.13	83.90	Uroporphyrinogen decarboxylase 2, chloroplastic
<i>Orange1.1t02279</i>	37.48	71.77	87.12	Coproporphyrinogen-III oxidase, chloroplastic
<i>Cs5g06770</i>	4.31	6.90	7.22	Oxygen-independent coproporphyrinogen-III oxidase 1
<i>Cs2g24910</i>	21.98	25.25	31.77	Protoporphyrinogen oxidase, chloroplastic/mitochondrial
<i>Orange1.1t01782</i>	35.37	56.42	53.75	Protoporphyrinogen oxidase, chloroplastic
<i>Cs9g13460</i>	44.52	5.36	17.65	Magnesium-chelatase subunit H
<i>Cs2g30990</i>	16.52	19.32	21.84	Magnesium-chelatase 67 kDa subunit
<i>Cs2g05100</i>	118.46	82.35	183.85	Magnesium-chelatase subunit ChII-1, chloroplastic
<i>Cs7g19710</i>	6.74	3.42	18.65	Magnesium-protoporphyrin O-methyltransferase
<i>Cs6g16200</i>	76.55	14.23	116.31	Magnesium-protoporphyrin IX monomethyl ester [oxidative] cyclase 1
<i>Cs1g06850</i>	22.97	15.00	167.60	Protochlorophyllide reductase A, chloroplastic
<i>Cs5g16830</i>	5.28	29.95	0.81	Chlorophyllase type 0
<i>Cs9g07520</i>	30.05	13.07	20.43	Chlorophyllase type 0
<i>Cs6g08720</i>	57.16	45.38	61.05	Bacteriochlorophyll synthase 34 kDa chain
<i>Cs3g19690</i>	47.34	3.63	10.36	Chlorophyll synthase, putative [ <i>Ricinus communis</i> ]
<i>Cs4g15890</i>	56.44	69.89	61.91	Chlorophyll (ide) b reductase NOL, chloroplastic
<i>Cs7g24010</i>	5.24	11.18	13.54	Chlorophyll (ide) b reductase NOL, chloroplastic
<i>Cs8g15480</i>	64.04	92.78	73.45	Pheophorbide a oxygenase, chloroplastic
<i>Cs1g22670</i>	37.78	73.56	82.11	Red chlorophyll catabolite reductase, chloroplastic

**Carotenoid biosynthesis**

<i>Cs6g15910</i>	79.73	216.13	172.64	Phytoene synthase
<i>Orange1.It02108</i>	30.15	85.62	32.83	PREDICTED: phytoene synthase 2, chloroplastic-like [ <i>Vitis vinifera</i> ]
<i>Orange1.It02361</i>	50.61	63.09	64.41	Phytoene dehydrogenase, chloroplastic/chromoplastic
<i>Cs5g24730</i>	47.11	59.11	58.21	15-cis-zeta-carotene isomerase, chloroplastic
<i>Cs3g11180</i>	56.36	81.36	70.96	Phytoene dehydrogenase, chloroplastic/chromoplastic
<i>Cs6g13340</i>	25.39	26.28	23.76	Prolycopene isomerase 1, chloroplastic
<i>Cs4g14850</i>	7.43	5.56	10.07	Capsanthin/capsorubin synthase, chromoplast
<i>Orange1.It00772</i>	9.33	8.65	11.12	Capsanthin/capsorubin synthase, chromoplast
<i>Orange1.It01058</i>	38.85	39.93	39.95	Cytochrome P450 97B1, chloroplastic
<i>Cs9g19270</i>	1038.75	1722.54	1359.83	Beta-carotene 3-hydroxylase 1, chloroplastic
<i>Cs1g22620</i>	65.41	82.35	95.98	3-hydroxybenzoate 6-hydroxylase 1
<i>Orange1.It04051</i>	1.01	0.95	1.10	3-hydroxybenzoate 6-hydroxylase 1
<i>Cs5g26080</i>	11.76	9.88	16.31	Violaxanthin de-epoxidase, chloroplastic
<i>Orange_new Gene_1755</i>	0.45	3.82	9.60	Lycopene beta-cyclase [ <i>Citrus×paradisi</i> ]

**ABA metabolism**

<i>Cs8g13780</i>	4.47	3.20	4.51	Indole-3-acetaldehyde oxidase
<i>Cs6g01180</i>	46.39	38.09	60.42	Xanthoxin dehydrogenase
<i>Cs2g03270</i>	2.08	67.84	18.90	9-cis-epoxycarotenoid dioxygenase 2 [ <i>Citrus sinensis</i> ]
<i>Cs5g14370</i>	28.65	20.09	8.45	Putative 9-cis-epoxycarotenoid dioxygenase 3 [ <i>Citrus sinensis</i> ]
<i>Cs7g14820</i>	2.18	0.26	5.90	Carotenoid cleavage dioxygenase 4a [ <i>Citrus clementina</i> ]
<i>Cs9g11260</i>	0.00	0.00	0.00	Carotenoid 9,10(9,10')-cleavage dioxygenase 1
<i>Cs6g19380</i>	60.57	30.48	9.86	ABA 8'-hydroxylase [ <i>Citrus sinensis</i> ]
<i>Cs8g05940</i>	2.05	3.80	3.20	Abscisic acid 8'-hydroxylase 1

---

<i>Cs8g18780</i>	1.10	0.78	0.27	ABA 8'&apos; -hydroxylase [ <i>Citrus sinensis</i> ]
------------------	------	------	------	--

---

234

235 According to the result of expression and annotation analyses, thirteen transcripts i.e. *BCHP*,  
 236 *CRD1*, *CHLM*, *CHLH1*, *HEMFI/HEMF2*, *FC1*, *DVR*, *CAO*, *CLH*, *CCS*, *PSY*, *AB* and *NCED1*  
 237 associated with chlorophyll metabolism, carotenoid biosynthesis and ABA metabolism were  
 238 obtained with a Fold Change  $\geq 2$  and FDR < 0.01 as screening standard (**Table 5**).

239

240

241 **Table 5** Analyses of DEGs associated with carotenoid biosynthesis, chlorophyll and ABA  
 242 metabolism

Gene ID	Symbols
<b>Chlorophyll metabolism</b>	
<i>Cs5g10740/ Cs2g26780</i>	Geranyl acyl geranyl acyl diphosphate reductase ( <i>BCHP</i> )
<i>Cs6g16200</i>	Methyl magnesium protoporphyrin IX single cyclase ( <i>CRD1</i> )
<i>Cs7g19710</i>	Magnesium protoporphyrin IX methyl transferase ( <i>CHLM</i> )
<i>Cs2g05100/ Cs9g13460</i>	Mg-chelatase subunit D ( <i>CHLD</i> )/Mg-chelatase subunit H ( <i>CHLH1</i> )
<i>Orange1.1t02279</i>	Coproporphyrin oxidative decarboxylase ( <i>HEMFI/HEMF2</i> )
<i>Cs4g18730</i>	Ferrochelatase ( <i>FC1</i> )
<i>Cs1g06850</i>	Divinyl reductase ( <i>DVR</i> )
<i>Cs3g19690</i>	Chlorophyllide a oxygenase ( <i>CAO</i> )
<i>Cs5g16830</i>	Chlorophyllase ( <i>CLH</i> )
<b>Carotenoid biosynthesis</b>	
<i>Orange_new Gene_1755</i>	Capsanthin/capsorubin synthase ( <i>CCS</i> )
<i>Orange1.1t02108/Cs6g15910</i>	Phytoene synthase ( <i>PSY</i> )
<b>ABA metabolism</b>	
<i>Cs3g23530</i>	Abscisic acid 8'-hydroxylase ( <i>AB</i> )

---

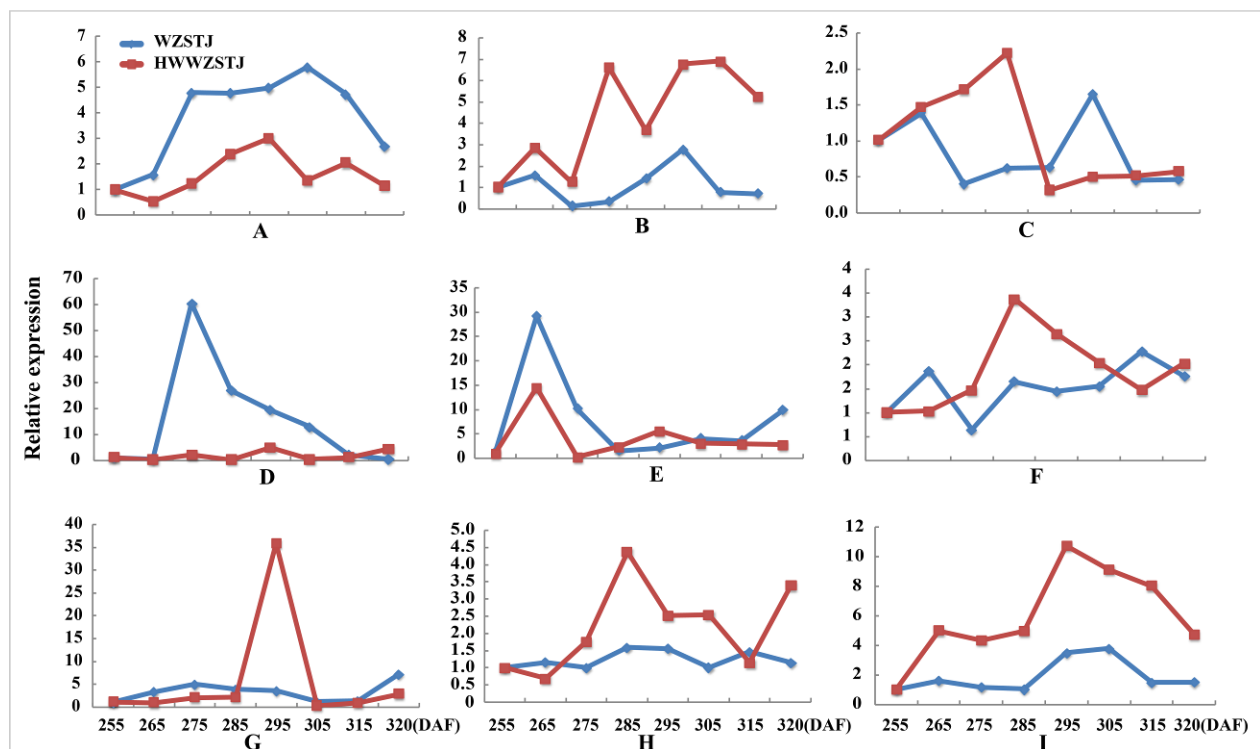
Cs5g14370

9-cis-epoxycarotenoid dioxygenase (*NCED1*)

243

## 244 Expression Analyses of Candidate Transcripts

245 Expression patterns of candidate transcripts associated with chlorophyll metabolism were  
 246 analyzed between WZSTJ and HWWZSTJ at all fruit maturation stages (**Fig. 3**). Compared with  
 247 WZSTJ, lower expression levels of *ALADI* and *CLH* were detected in HWWZSTJ at all fruit  
 248 maturation stages. Expression of *ALADI* and *CLH* were increasing before fruit maturation and  
 249 decreased thereafter in both WZSTJ and HWWZSTJ. The highest expression level of *CLH* was  
 250 detected on the 295<sup>th</sup> DAF in HWWZSTJ, which was 20 d later than WZSTJ. Expression levels  
 251 of *CAOI* and *PAO* in HWWZSTJ was higher than that in WZSTJ. *FCI* showed a decrease trend  
 252 during fruit maturation of WZSTJ and HWWZSTJ. As for *GluRS*, *CHLHI*, *HEMG* and *CHLM*,  
 253 they showed irregular expression patterns in WZSTJ and HWWZSTJ (**Fig. 3**).



254

255 **Figure 3** Expression patterns of genes associated with chlorophyll metabolism in WZSTJ  
 256 and HWWZSTJ at all fruit maturation stages

257

A, *ALADI*; B, *CAOI*; C, *CHLM*; D, *CLH*; E, *FCI*; F, *GluRS*; G, *HEMF1*; H, *HEMG*; I,

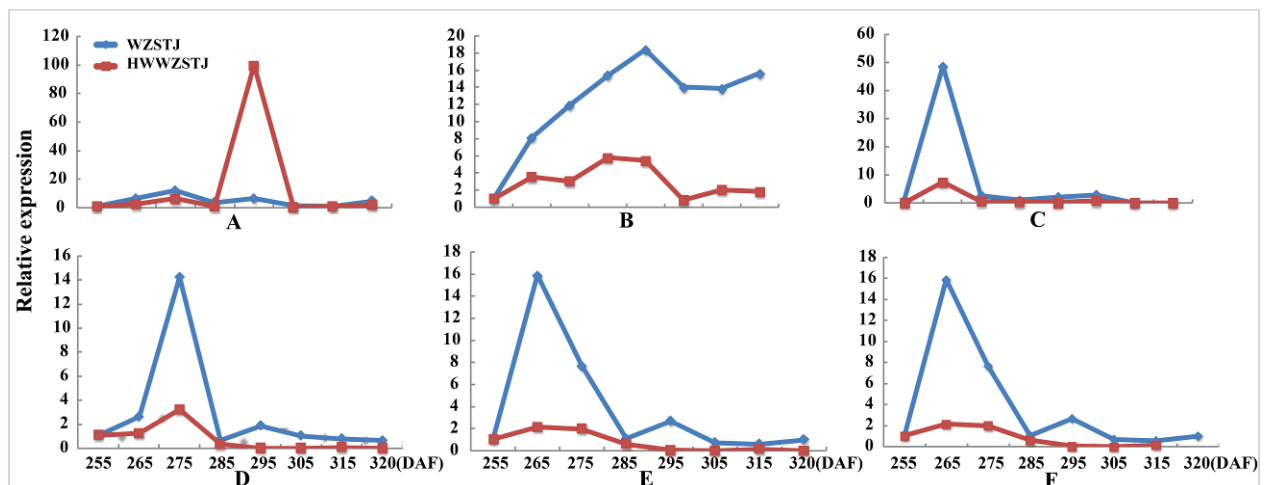
258

PAO

259

260 Six carotenoid biosynthesis-related transcripts showed a trend from rise to decline at all  
 261 fruit maturation stages of WZSTJ and HWWZSTJ (**Fig. 4**). The highest expression level of *CCS*  
 262 was detected on the 295<sup>th</sup> DAF in HWWZSTJ which was 20 d later than that of WZSTJ.  
 263 Expression levels of *PDS1*, *PSY3*, *PSY5*, *PSY6* and *PSY7* in WZSTJ were higher than that of  
 264 HWWZSTJ. *PDS1* showed an increasing trend during fruit maturing of WZSTJ and HWWZSTJ  
 265 and reached its maximum expression on the 295<sup>th</sup> DAF. *PSY5* showed the highest expression  
 266 levels on the 275<sup>th</sup> DAF compared to the highest expression levels of *PSY3*, *PSY6* and *PSY7* on  
 267 the 265<sup>th</sup> DAF in both WZSTJ and HWWZSTJ. Expression levels of *PSY5* were increasing  
 268 before the 275<sup>th</sup> DAF and decreased thereafter. *PSY3*, *PSY6* and *PSY7* were up-regulation before  
 269 the 265<sup>th</sup> DAF and decreased gradually thereafter (**Fig. 4**).

270



271

272 **Figure 4** Expression patterns of genes associated with carotenoid biosynthesis in WZSTJ

273 and HWWZSTJ at all fruit maturation stages

274 A, *CCS*; B, *PDS1*; C, *PSY3*; D, *PSY5*; E, *PSY6*; F, *PSY7*

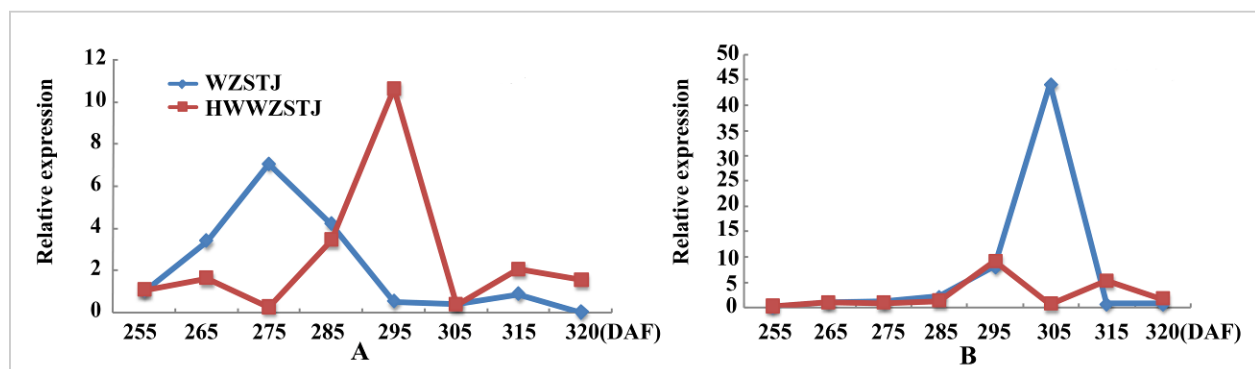
275

276 Expression patterns of two candidate transcripts i.e. *ABI* and *NCED1* related to ABA  
 277 metabolism were analyzed at all fruit maturation stages of WZSTJ and HWWZSTJ (**Fig. 5**). *ABI*

278 showed a trend from rise to decline during fruit maturation stages of WZSTJ and HWWZSTJ.  
 279 The highest expression level of *ABI* was obtained on the 295<sup>th</sup> DAF in HWWZSTJ, which was  
 280 20 d later than WZSTJ. Similar expression patterns of *NCEDI* were observed before the 295<sup>th</sup>  
 281 DAF in HWWZSTJ and WZSTJ (**Fig. 5**). The expression level of *NCEDI* in HWWZSTJ was  
 282 lower than that of WZSTJ during 275<sup>th</sup> DAF to 305<sup>th</sup> DAF. The highest expression level of  
 283 *NCEDI* was detected on the 305<sup>th</sup> DAF of WZSTJ and significantly decreased thereafter (**Fig. 5**).  
 284 However, the highest expression of *NCEDI* was at 295 DAF in HWWZSTJ. Results from  
 285 expression analyses of candidate genes suggested that *NCEDI* might play a leading role in late-  
 286 maturing characteristics of HWWZSTJ.

287

288



289

290 **Figure 5** Expression patterns of transcripts associated with ABA metabolism in WZSTJ and  
 291 HWWZSTJ at all fruit maturation stages

291

292

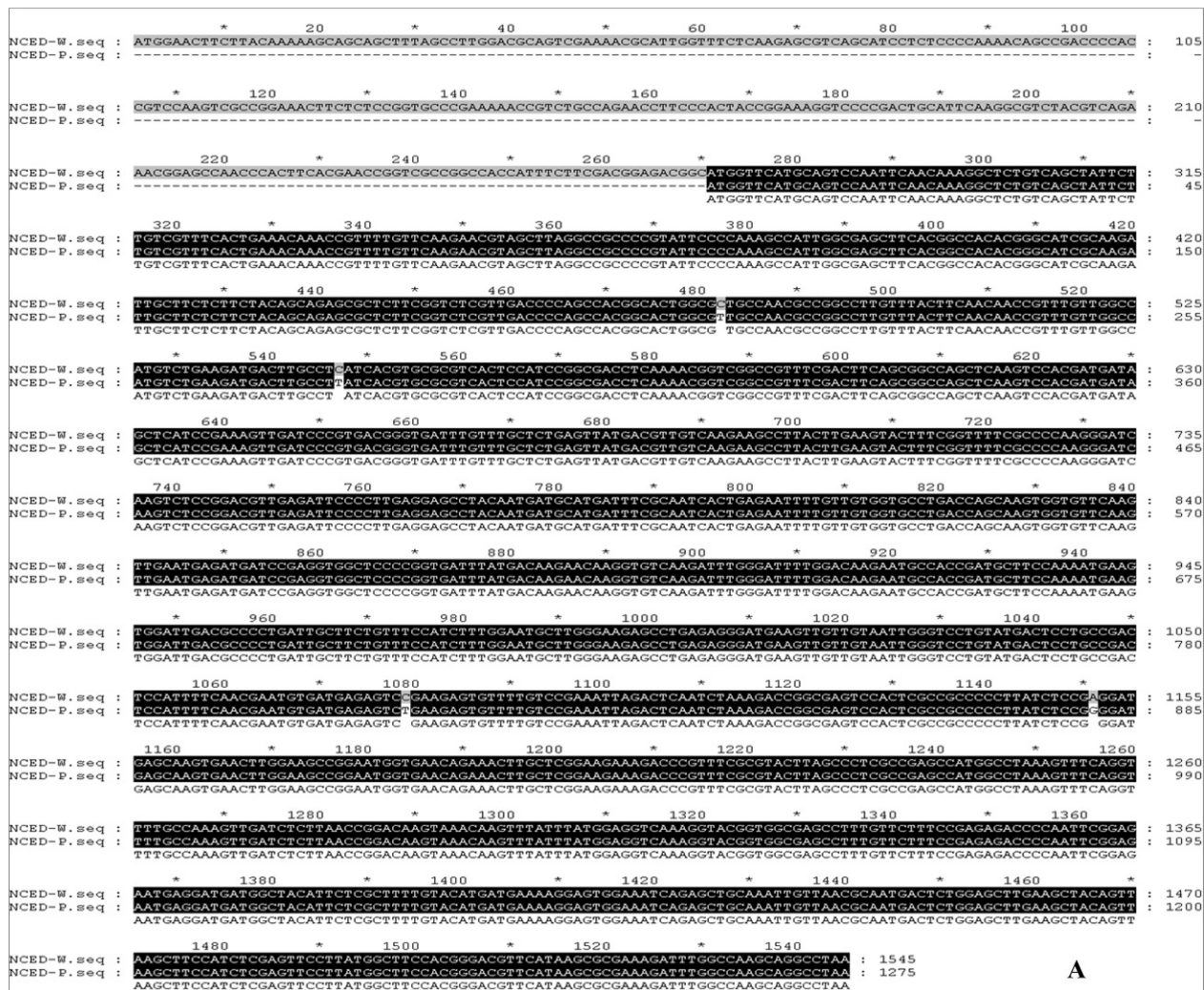
A, *ABI*; B, *NCEDI*

293

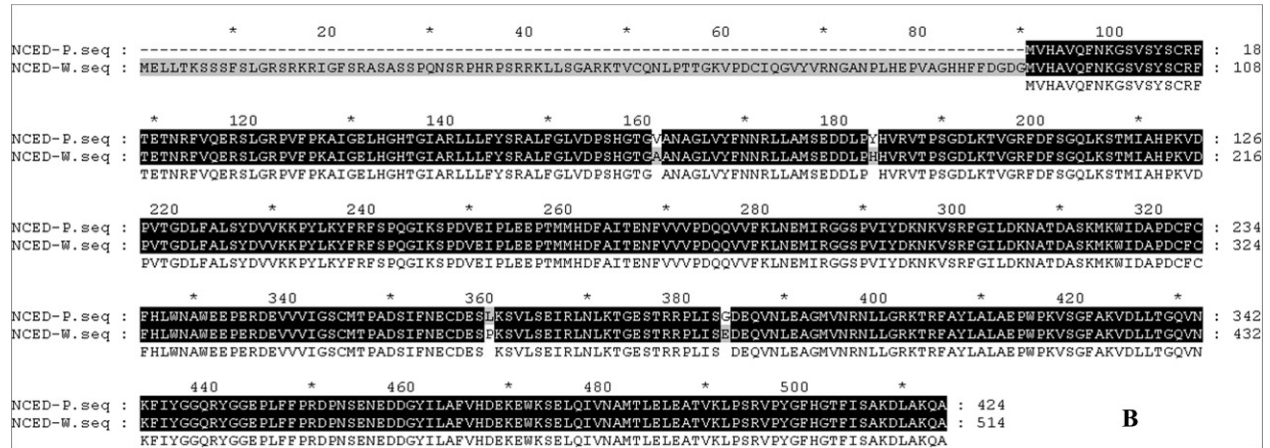
#### 294 Cloning and Phylogenetic Analyses of Candidate Genes

295 Full-length cDNA sequences of *CLH* and *DVR* from chlorophyll metabolism, *PSY3*, *PSY5*,  
 296 *PSY6*, *PSY7* and *CCS* from carotenoid biosynthesis, *ABI* and *NCEDI* from ABA metabolism  
 297 were cloned from HWWZSTJ and WZSTJ mandarins. There was one difference in base pair of  
 298 *CLH*, *PSY3* and *PSY5* cDNA sequences between HWWZSTJ and WZSTJ (**Fig. S5-7**). However,  
 299 the amino acid sequences of *CLH*, *PSY3* and *PSY5* from HWWZSTJ was 100% identical to that

300 from WZSTJ. There were 4, 6, 4, 3 and 17 bp difference between the sequences of *DVR*, *CCS*,  
 301 *PSY6*, *PSY7* and *ABI* derived from HWWZSTJ and WZSTJ and this resulted in 2, 3, 3, 1 and 8  
 302 differences in the amino acids that would have been incorporated during translation of these  
 303 transcripts (**Fig. S8-12**). Compared with WZSTJ, there were 270 consecutive bases missing in  
 304 cDNA sequence of the *NCEDI* from HWWZSTJ (**Fig. 6**). Phylogenetic analysis showed that  
 305 *CLH*, *DVR*, *PSY* and *NCEDI* belonged to the same cluster, and their homology in comparison  
 306 with similar sequences derived from other species is depicted in **Fig. S13-16**. Results from  
 307 sequence analyses suggested that deletion of 270 nucleotides in *NCEDI* maybe result in late-  
 308 maturing characteristics of HWWZSTJ.



309



310

311 **Figure 6** Alignments of cDNA (A) and amino acid (B) sequences of the *NCEDI* from

312 HWWZSTJ and WZSTJ

313 W, HWWZSTJ; P, WZSTJ

314

315 **Discussion**

316 Chlorophyll degradation, carotenoid biosynthesis and ABA metabolism play important roles  
 317 in regulating citrus fruit maturation through a series of related genes or special signal network  
 318 (Zhang et al., 2014). In this study, RNA-Seq technology was used to screen DEGs between a late-  
 319 maturing mandarin mutant HWWZSTJ and its wild type WZSTJ during fruit maturation. DEGs  
 320 between any two of the three libraries were significantly enriched in biological processes such as  
 321 photosynthesis, phenylpropanoid biosynthesis, carotenoid biosynthesis, chlorophyll metabolism,  
 322 ABA metabolism, starch and sucrose metabolism (**Table 3**). Thirteen maturing-related genes  
 323 involved in carotenoid biosynthesis, chlorophyll degradation and ABA metabolism were selected  
 324 for further analysis.

325 CLH is the key enzyme catalyzing the first step in the chlorophyll degradation. It can  
 326 catalyze the hydrolysis of ester bond to yield chlorophyllide and phytol in the chlorophyll  
 327 breakdown pathway (Jacob-Wilk et al., 1999; Tsuchiya & Takamiya, 1999). Jacob-Wilk et al  
 328 isolated a CLH encoding an active chlorophyllase enzyme and verified the role of CLH in  
 329 chlorophyll dephytylation by *in vitro* recombinant enzyme assays. Expression level of *CLH* in  
 330 Valencia orange peel was low and constitutive and did not significantly increase during fruit

331 development and ripening (Jacob-Wilk et al., 1999). In the present study, a *CLH* was obtained  
332 from the transcriptome dataset. No difference was detected in the amino acid sequences of *CLH*  
333 between HWWZSTJ and WZSTJ. Expression levels of *CLH* were increasing prior to citrus fruit  
334 maturing, decreasing thereafter in both WZSTJ and HWWZSTJ. The highest expression level of  
335 *CLH* was detected on the 295<sup>th</sup> DAF in HWWZSTJ, which was 20 d later than that of WZSTJ  
336 (**Fig. 3**). Similar results were also observed in peels of the late-maturing mutant from Fengjie72-  
337 1 navel orange (Liu et al., 2006) and Tardivo clementine mandarin (Distefano et al., 2009).  
338 Those results suggested that CLH may balance between chlorophyll synthesis and its breakdown  
339 (Jacob-Wilk et al., 1999).

340 Citrus is a complex source of carotenoids with the largest number of carotenoids (Kato,  
341 2004). Carotenoid contents and compositions are main factors that affect peel color of most  
342 citrus fruits (Tadeo et al., 2008). *PSY* is a regulatory enzyme in carotenoid biosynthesis (Welsch  
343 et al., 2000). *PSY* is present at low expression level in unripe (green) melon fruit, reaches its  
344 highest levels when the fruit turns from green to orange and persists at lower levels during later  
345 ripening stages (Karvouni et al., 1995). Liu et al (2006) studied the mechanism underlying the  
346 difference between Fengwan (a late-maturing mutant) navel orange and its original cultivar  
347 (Fengjie72-1). The highest expression levels of some carotenoid biosynthetic enzymes in the  
348 peels of the late-maturing mutant occurred 30 d later than that of the original cultivar (Liu et al.,  
349 2006). In this work, *PSY* showed a trend from rise to decline at all fruit maturation stages of the  
350 late-maturing mutant HWWZSTJ and its original line WZSTJ. The expression levels of *PSY3*,  
351 *PSY5*, *PSY6* and *PSY7* in HWWZSTJ were lower than that in WZSTJ. These results  
352 demonstrated that the mutation in HWWZSTJ influenced the transcriptional activation of *PSY*.

353 ABA can be considered as a ripening regulator during fruit maturation and ripening. *NCED*,  
354 a key enzyme involved in ABA biosynthesis, plays an important role in fruit ripening of avocado  
355 (*Persea americana*) (Chernys and Zeevaart, 2007), orange (*Citrus sinensis*) (Rodrigo et al.,  
356 2006), tomato (*Solanum lycopersicum*) (Nitsch et al., 2009; Zhang et al., 2009b), grape (*Vitis*  
357 *vinifera*) and peach (*Prunus persica*) (Zhang et al., 2009a). The *NCED1* were expressed only at

358 the onset stage of ripening in peach and grape, when ABA content became high (Zhang et al.,  
359 2009a). Zhang et al. (2014) studied the mechanism of a spontaneous late-maturing mutant of  
360 ‘Jincheng’ sweet orange and its wild type through the comparative analysis. The highest  
361 expression of *CsNCEDI* was at 215 DAA in WT. In our study, expression levels of *NCEDI*  
362 increased prior to fruit maturing and decreased significantly thereafter in both HWWZSTJ and  
363 WZSTJ. The highest expression level of *NCEDI* was detected on the 305<sup>th</sup> DAF of WT  
364 (WZSTJ). Our results were consistent with previous findings that *NCEDI* plays the most  
365 important role in the ABA biosynthesis pathway during the fruit maturing process (Zhang et al.,  
366 2014). Deletion of nucleotides could cause a shift of the reading frame and truncated protein,  
367 which can result in natural mutants. Compared with cDNA sequence of *NCEDI* from WZSTJ,  
368 there were 270 consecutive bases missing in HWWZSTJ (**Fig. 6**). Those results suggested that  
369 *NCEDI* might play an important role in late-maturing of HWWZSTJ. A high-efficient  
370 regeneration system for WZSTJ has been established (Wang et al., 2015) and further study on  
371 the role of *NCEDI* in citrus is being carried out through genetic engineering.

372

### 373 **Conclusion**

374 RNA-Seq technology was used to identify pigment-related genes from a late-maturing  
375 mandarin mutant HWWZSTJ and its original cultivar WZSTJ. Thirteen candidate transcripts  
376 related to chlorophyll metabolism, carotenoid biosynthesis and ABA metabolism were obtained.  
377 *NCEDI*, a gene involved in ABA metabolism, is probably involved in the formation of late  
378 maturity of HWWZSTJ based on sequence and expression analyses. The present study opens up  
379 a new perspective to study the formation of late maturity in citrus fruit.

### 380 **Acknowledgements**

381 We thank Peng Li, Zixing Ye and Jietang Zhao for help and support with field management  
382 and technical assistance.

383

### 384 **REFERENCES**

385 Altschul, S.; Madden, T.; Schäffer, A.A.; Zhang, J.; Zhang, Z.; Miller, W.; Lipman, D.J. 1997. Gapped

- 386 BLAST and PSI-BLAST, A new generation of protein database search programs. *Nucleic Acids Research*  
387 25: 3389-3402.
- 388 **Bastías, A., López-Climent, M., Valcárcel, M., Rosello, S., Gómez-Cadenas, A., Casaretto, J.A. 2011.**  
389 Modulation of organic acids and sugar content in tomato fruits by an abscisic acid-regulated transcription  
390 factor. *Physiologia Plantarum* 141: 215-226.
- 391 **Chernys, J.T.; Zeevaart, J.A.D. 2007.** Characterization of the 9-cis-epoxycarotenoid dioxygenase gene  
392 family and the regulation of abscisic acid biosynthesis in avocado. *Plant Physiology* 124: 343–353.
- 393 **Deng, Y.Y.; Li, J.Q, Wu, S.F.; Zhu Y.P.; Chen, Y.W.; He, F.C. 2006.** Integrated nr database in protein  
394 annotation system and its localization. *Computer Engineering* 5: 71–74.
- 395 **Distefano, G.; Casas, G.; Caruso, M.; Todaro A.; Rapisarda Paolo.; La Malfa S.; Gentile A.; Tribulato**  
396 **E. 2009.** Physiological and molecular analysis of the maturation process in fruits of clementine mandarin  
397 and one of its late-ripening mutants. *Journal of Agricultural and Food Chemistry* 57: 7974–7982.
- 398 **FAOSTAT. 2014.** [http://faostat.fao.org/site/567/DesktopDefault.aspx?PageID\\$=\\$567#ancor](http://faostat.fao.org/site/567/DesktopDefault.aspx?PageID$=$567#ancor).
- 399 **Ghosh, S.; Meli, V.S.; Kumar, A.; Thakur, A.; Chakraborty, N.; Chakraborty, S.; Datta, A. 2011.** The  
400 N-glycan processing enzymes  $\alpha$ -mannosidase and  $\beta$ -D-N-acetylhexosaminidase are involved in ripening-  
401 associated softening in the non-climacteric fruits of capsicum. *Journal of Experimental Botany* 62(2):  
402 571–582
- 403 **Harris, M.A.; Clark, J.; Ireland, A.; Lomax, J.; Ashburner, M.; Foulger, R.; Eilbeck, K.; Lewis, S.;**  
404 **Marshall, B.; Mungall, C.; Richter, J.; Rubin, G.M.; Blake, J.A.; Bult, C.; Dolan, M.; Drabkin, H.;**  
405 **Eppig, J.T.; Hill, D.P.; Ni, L.; Ringwald, M.; Balakrishnan, R.; Cherry, J.M.; Christie, K.R.;**  
406 **Costanzo, M.C.; Dwight, S.S.; Engel, S.; Fisk, D.G.; Hirschman, J.E.; Hong, E.L.; Nash, R.S.;**  
407 **Sethuraman, A.; Theesfeld, C.L.; Botstein, D.; Dolinski, K.; Feierbach, B.; Berardini, T.; Mundodi,**  
408 **S.; Rhee, S.Y.; Apweiler, R.; Barrell, D.; Camon, E.; Dimmer, E.; Lee, V.; Chisholm, R.; Gaudet, P.;**  
409 **Kibbe, W.; Kishore, R.; Schwarz, E.M.; Sternberg, P.; Gwinn, M.; Hannick, L.; Wortman, J.;**  
410 **Berriman, M.; Wood, V.; de la Cruz, N.; Tonellato, P.; Jaiswal, P.; Seigfried, T.; White, R. 2004.**  
411 The Gene Ontology (GO) database and informatics resource. *Nucleic Acids Research* 32: 258–261
- 412 **Jacob-Wilk, D.; Holland, D.; Goldschmidt, E.E.; Riov, J.; Eyal, Y. 1999.** Chlorophyll breakdown by

- 413 chlorophyllase, Isolation and functional expression of the *Chlase1* gene from ethylene-treated *Citrus* fruit  
414 and its regulation during development. *Plant Journal* 20: 653–661.
- 415 **Jia, H.F.; Chai, Y.M.; Li, C.J.; Lu, D.; Luo, J.J.; Qin, L.; Shen, Y.Y. 2011.** Abscisic acid plays an  
416 important role in the regulation of strawberry fruit ripening. *Plant Physiology* 157 : 188–199.
- 417 **Kanehisa, M.; Goto, S.; Kawashima, S.; Okuno, Y.; Hattori, M. 2004.** The KEGG resource for deciphering  
418 the genome. *Nucleic Acids Research* 32: 277–280.
- 419 **Karppinen, K.; Hirvela, E.; Nevala, T.; Sipari, N.; Suokas, M.; Jaakola, L. 2013.** Changes in the abscisic  
420 acid levels and related gene expression during fruit development and ripening in bilberry (*Vaccinium*  
421 *myrtillus* L.). *Phytochemistry* 95: 127–134.
- 422 **Karvouni, Z.; John, I.; Taylor, J.; Watson, C.F.; Turner, A.J.; Grierson, D. 1995.** Isolation and  
423 characterisation of a melon cDNA clone encoding phytoene synthase. *Plant Molecular Biology* 27: 1153–  
424 1162.
- 425 **Kato, M.; Ikoma, Y.; Matsumoto, H.; Kuniga, T.; Nakajima, N.; Yoshida, T.; Yano, M. 2004.**  
426 Accumulation of carotenoids and expression of carotenoid biosynthetic genes during maturation in citrus  
427 fruit. *Plant Physiology* 134: 824–837.
- 428 **Koyama, K.; Sadamatsu, K.; Goto-Yamamoto, N. 2010.** Abscisic acid stimulated ripening and gene  
429 expression in berry skins of the *Cabernet Sauvignon* grape. *Functional & Integrative Genomics* 10: 367-  
430 381.
- 431 **Kumar, R.; Khurana, A.; Sharma, A.K. 2014.** Role of plant hormones and their interplay in development  
432 and ripening of fleshy fruits. *Journal of Experimental Botany* 65: 4561–4575.
- 433 **Leng, P.; Zhang, G.L.; Li, X.X.; Wang, L.H.; Zheng, Z.M. 2009.** Cloning of 9-cis-epoxycarotenoid  
434 dioxygenase (NCED) gene encoding a key enzyme during abscisic acid (ABA) biosynthesis and ABA  
435 regulated ethylene production in detached young persimmon calyx. *Chinese Science Bulletin* 54: 2830–  
436 2838.
- 437 **Liu, Y.; Tang, P.; Tao, N.; Xu, Q.; Peng S.A.; Deng X.X.; Xiang K.S.; Huang, R.H. 2006.** Fruit coloration  
438 difference between Fengwan, a late-maturing mutant and its original cultivar Fengjie 72-1 of Navel  
439 Orange (*Citrus sinensis* Osbeck). *Zhiwu Shengli yu Fenzi Shengwuxue Xuebao* 32: 31–36.

- 440 **Liotenberg S, North H, Marion-Poll A. 1999.** Molecular biology and regulation of abscisic acid biosynthesis  
441 in plants. *Plant Physiology and Biochemistry* 37: 341–350.
- 442 **Livak, K.J.; Schmittgen, T.D. 2011.** Analysis of relative gene expression data using real-time quantitative  
443 PCR and the  $2^{-\Delta\Delta CT}$  method. *Methods* 25: 402–408.
- 444 **Luchi S1, Kobayashi M, Taji T, Naramoto M, Seki M, Kato T, Tabata S, Kakubari Y, Yamaguchi-**  
445 **Shinozaki K, Shinozaki K. 2001.** Regulation of drought tolerance by gene manipulation of 9-cis-  
446 epoxy-carotenoid dioxygenase, a key enzyme in abscisic acid biosynthesis in *Arabidopsis*. *Plant Journal*  
447 27: 325–333.
- 448 **Nicolas, P.; Lecourieux, D.; Kappel, C.; Cluzet, S.; Cramer G.; Delrot S.; Lecourieux F. 2014.** The bZIP  
449 transcription factor *VvABF2* is an important transcriptional regulator of ABA-dependent grape berry  
450 ripening processes. *Plant Physiology* 164: 365–383.
- 451 **Nitsch, L.; Oplaat, C.; Feron, R.; Ma, Q.; Wolters-Arts, M.; Hedden, P.; Mariani, C.; Vriezen, W.H.**  
452 **2009.** Abscisic acid levels in tomato ovaries are regulated by *LeNCED1* and *SICYP707A1*. *Planta* 229:  
453 1335–1346.
- 454 **Qin, Y.H.; Li, G.Y.; Wang, L.; Jaime, A.; Ye, Z.X.; Feng, Q.R.; Hu, G.B. 2015.** A comparative study  
455 between a late-ripening mutant of citrus and its original line in fruit coloration, sugar and acid metabolism  
456 at all fruit maturation stage. *Fruits* 70: 5–11.
- 457 **Qin, Y.H.; Ye, Z.X.; Hu, G.B.; Li, G.Y.; Chen, J.Z.; Lin, S.Q. 2013.** ‘Huawan Wuzi Shatangju’, a late-  
458 maturing mandarin cultivar. *Acta Horticulturae Sinica* 40:1411–1412.
- 459 **Rodrigo, M.J.; Alquezar, B.; Zacarías, L. 2006.** Cloning and characterization of two 9-cis-epoxycarotenoid  
460 dioxygenase genes, differentially regulated during fruit maturation and under stress conditions, from  
461 orange (*Citrus sinensis* L. Osbeck). *Journal of Experimental Botany* 57: 633–643.
- 462 **Romero, P.; Lafuente, M.T.; Rodrigo, M.J. 2012.** The *Citrus* ABA signalosome, identification and  
463 transcriptional regulation during sweet orange fruit ripening and leaf dehydration. *Journal of*  
464 *Experimental Botany* 63: 4931-4945.
- 465 **Soto, A.; Ruiz, K.; Ravaglia, D.; Costa, G.; Torrigiani, P. 2013.** ABA may promote or delay peach fruit  
466 ripening through modulation of ripening and hormone-related gene expression depending on the

- 467 developmental stage. *Plant Physiology and Biochemistry* 64: 11–24.
- 468 **Sun, L.; Sun, Y.F.; Zhang, M.; Wang, L.; Ren, J.; Cui, M.; Wang, Y.P.; Ji, K.; Li, P.; Li, Q.; Chen, P.;**  
469 **Dai, S.J.; Duan, C.R.; Wu, Y.; Leng, P. 2012.** Suppression of 9-cis-Epoxycarotenoid dioxygenase,  
470 which encodes a key enzyme in abscisic acid biosynthesis, alters fruit texture in transgenic tomato. *Plant*  
471 *Physiology* 158: 283–298.
- 472 **Sun, L.; Wang, Y.P.; Chen, P.; Ren, J.; Ji, K.; Li, Q.; Li, P.; Dai, S.J.; Leng, P. 2011.** Transcriptional  
473 regulation of *SIPYL*, *SIPP2C*, and *SISnRK2* gene families encoding ABA signal core components during  
474 tomato fruit development and drought stress. *Journal of Experimental Botany* 62: 5659–5669.
- 475 **Sun, L.; Zhang, M.; Ren, J.; Qi, J.; Zhang, G.; Leng P. 2010.** Reciprocity between abscisic acid and  
476 ethylene at the onset of berry ripening and after harvest. *BMC Plant Biology* 10: 257–268.
- 477 **Tadeo, F.R.; Cercos, M.; Colmenero-Flores, J.M.; Iglesias, D.J.; Naranjo, M.A.; Rios, G.; Carrera, E.;**  
478 **Ruiz-Rivero, O.; Lliso, I.; Morillon, R.; Ollitrault, P.; Talon, M. 2008.** Molecular physiology of  
479 development and quality of citrus. *Advances in Botanical Research* 47: 147–223.
- 480 **Tatusov, R.; Galperin, M.; Natale, D.; Koonin, E.V. 2000.** The COG database, A tool for genome-scale  
481 analysis of protein functions and evolution. *Nucleic Acids Research* 28: 33–36.
- 482 **Trapnell, C., Pachter, L., Salzberg, S.L. 2009.** TopHat: discovering splice junctions with RNA-Seq.  
483 *Bioinformatics* 25: 1105–1111
- 484 **Tsuchiya, T.; Takamiya, K.I. 1999.** Cloning of chlorophyllase, the key enzyme in chlorophyll degradation,  
485 finding of a lipase motif and the induction by methyl jasmonate. *Proceedings of the National Academy of*  
486 *Sciences of the United States of America* 96: 15362–15367.
- 487 **Wang, L.; Li, P.; Su, C.L.; Ma, Y.W.; Yan, L.; Hu, G.B.; Qin, Y.H. 2015.** Establishment of a high-efficient  
488 regeneration system for Wuzhishatangju. *South China Fruits* 44: 48–51.
- 489 **Wang, X.H., Yin, W., Wu, J.X., Chai, L.J., Yi, H.L. 2016.** Effects of exogenous abscisic acid on the  
490 expression of citrus fruit ripening-related genes and fruit ripenin. *Scientia Horticulturae* 201: 175–183
- 491 **Wang J, Chen DJ, Lei Y, Chang JW, Hao BH, Xing F, Li S, Xu Q, Deng XXin, Chen LL.**  
492 **2014.** *Citrus sinensis* annotation project (CAP): a comprehensive database for sweet orange  
493 genome. *PLoS ONE* 9: e87723.

494 **Wang, Y.P.; Wang, Y.; Ji, K.; Dai, S.J.; Hu, Y.; Sun, L.; Li, Q.; Chen, P.; Sun, Y.F.; Duan, C.R.; Wu, Y.;**  
495 **Luo, H.; Zhang, D.; Guo, Y.D.; Leng, P. 2013.** The role of abscisic acid in regulating cucumber fruit  
496 development and ripening and its transcriptional regulation. *Plant Physiology and Biochemistry* 64: 70–79.

497 **Welsch, R.; Beyer, P.; Huguency, P.; Kleinig, H.; von Lintig, J. 2000.** Regulation and activation of  
498 phytoene synthase, a key enzyme in carotenoid biosynthesis, during photomorphogenesis. *Planta* 211:  
499 846–854.

500 **Xu, Q.; Chen, L.L.; Ruan, X.; Chen, D.; Zhu, A.; Chen, C.; Bertrand, D.; Jiao, W.B.; Hao, B.H.; Lyon,**  
501 **M.P.; Chen, J.; Gao, S.; Xing, F.; Lan, H.; Chang, J.W.; Ge, X.; Lei, Y.; Hu, Q.; Miao, Y.; Wang, L.;**  
502 **Xiao, S.; Biswas, M.K.; Zeng, W.; Guo, F.; Cao, H.; Yang, X.; Xu, X.W.; Cheng, Y.J.; Xu, J.; Liu,**  
503 **J.H.; Luo, O.J.; Tang, Z.; Guo, W.W.; Kuang, H.; Zhang, H.Y.; Roose, M.L.; Nagarajan, N.; Deng,**  
504 **X.X.; Ruan, Y. 2013.** The draft genome of sweet orange (*Citrus sinensis*). *Nature Genetics* 45: 59–66.

505 **Zhang, M.; Leng, P.; Zhang, G.; Li, X. 2009a.** Cloning and functional analysis of 9-cis-epoxycarotenoid  
506 dioxygenase (NCED) genes encoding a key enzyme during abscisic acid biosynthesis from peach and  
507 grape fruits. *Journal of Plant Physiology* 166: 1241–1252.

508 **Zhang, M.; Yuan, B.; Leng, P. 2009b.** The role of ABA in triggering ethylene biosynthesis and ripening of  
509 tomato fruit. *Journal of Experimental Botany* 60: 1579–1588.

510 **Zhang, Y.; Wang, X.; Wu, J. 2014.** Comparative transcriptome analyses between a spontaneous late-ripening  
511 sweet orange mutant and its wild type suggest the functions of ABA, sucrose and JA during citrus fruit  
512 ripening. *PLoS ONE* 9: e116056.

513  
514